

A numerical simulation of hole and electron trapping due to radiation in silicon dioxide

V. Vasudevan and J. Vasi

Citation: *Journal of Applied Physics* **70**, 4490 (1991); doi: 10.1063/1.349083

View online: <http://dx.doi.org/10.1063/1.349083>

View Table of Contents: <http://scitation.aip.org/content/aip/journal/jap/70/8?ver=pdfcov>

Published by the [AIP Publishing](#)

Articles you may be interested in

[Numerical Simulation of Diffusion of Electrons and Holes in Shocked Silicon](#)

AIP Conf. Proc. **706**, 267 (2004); 10.1063/1.1780232

[Electron spin resonance investigation of hole trapping in reoxidized nitrided silicon dioxide](#)

J. Appl. Phys. **72**, 820 (1992); 10.1063/1.351823

[Radiation induced electron traps in silicon dioxide](#)

J. Appl. Phys. **54**, 6443 (1983); 10.1063/1.331924

[Interface trap generation in silicon dioxide when electrons are captured by trapped holes](#)

J. Appl. Phys. **54**, 2540 (1983); 10.1063/1.332323

[Hole traps in silicon dioxide](#)

J. Appl. Phys. **47**, 1082 (1976); 10.1063/1.322730

The advertisement features a blue background with a film strip graphic on the left. The text is in white and orange. The main headline reads 'Not all AFMs are created equal' in orange, followed by 'Asylum Research Cypher™ AFMs' in white, and 'There's no other AFM like Cypher' in orange. At the bottom, the website 'www.AsylumResearch.com/NoOtherAFMLikeIt' is listed in white. The Oxford Instruments logo, consisting of the word 'OXFORD' above 'INSTRUMENTS' in a white box, is in the bottom right corner, with the tagline 'The Business of Science®' below it.

Not all AFMs are created equal
Asylum Research Cypher™ AFMs
There's no other AFM like Cypher

www.AsylumResearch.com/NoOtherAFMLikeIt

OXFORD
INSTRUMENTS
The Business of Science®

A numerical simulation of hole and electron trapping due to radiation in silicon dioxide

V. Vasudevan and J. Vasi

Electrical Engineering Department, Indian Institute of Technology, Bombay 400076, India

(Received 6 June 1991; accepted for publication 9 July 1991)

The one-dimensional Poisson, continuity, and the trap rate equations are solved numerically to study the buildup of charge in silicon dioxide due to radiation. The flat-band voltage shift (ΔV_{fb}) is obtained as a function of total dose, the oxide thickness, the applied gate voltage, and the centroid of the trap distribution. The effect of including electron traps is studied. The results of the simulation are found to compare well with experimental data.

I. INTRODUCTION

One of the main effects of radiation incident on the metal-oxide-semiconductor (MOS) structure is the buildup of positive charge in the oxide. This is believed to occur due to the trapping of holes that are generated during radiation. Some insight into this process can be obtained from analytical solutions of the trap rate and the continuity equations in SiO_2 .¹ But this is not complete, as several approximations have to be made in order to get these solutions. A more accurate picture can be obtained through a numerical solution of the relevant equations in the oxide. In a series of papers,²⁻⁴ Holstrom *et al.* have reported some results of such numerical simulations. However, they have not included in their model effects like detrapping of holes, electron trapping, and geminate recombination, which we believe play a significant role in the buildup of positive charge. We have done a one-dimensional numerical simulation of the trapping process including these processes. This paper presents the results of this simulation, through which a physical understanding of various phenomena that occur during the buildup of positive charge in the oxide can be obtained.

II. NUMERICAL SOLUTIONS

Numerical solutions were carried out assuming that the Si-SiO₂ system is an abrupt heterojunction, with SiO₂ modeled as a wide-band-gap semiconductor. In this case the one-dimensional equations to be solved in the oxide are

$$\frac{d^2\psi}{dx^2} = \frac{-q}{\epsilon_{ox}} (p + p_T - n - n_T),$$

$$\frac{dp}{dt} = -\frac{1}{q} \frac{dJ_p}{dx} + G_{ox} - \frac{dp_T}{dt},$$

$$\frac{dn}{dt} = \frac{1}{q} \frac{dJ_n}{dx} + G_{ox} - \frac{dn_T}{dt},$$

$$\frac{dp_T}{dt} = \sigma_p v_{th} p (N_{Tp} - p_T) - \frac{p_T}{\tau_p},$$

$$\frac{dn_T}{dt} = \sigma_n v_{th} n (N_{Tn} - n_T) - \frac{n_T}{\tau_n} - \sigma_n v_{th} n p_T,$$

and in the semiconductor are

$$\frac{d^2\psi}{dx^2} = \frac{-q}{\epsilon_{si}} (D + p - n), \quad D = N_d^+ - N_a^-,$$

$$\frac{dp}{dt} = -\frac{1}{q} \frac{dJ_p}{dx} + G_{si} - R_{SRH},$$

$$\frac{dn}{dt} = \frac{1}{q} \frac{dJ_n}{dx} + G_{si} - R_{SRH}.$$

In the above equations,

$$J_p = q p \mu_p E - q D_p \frac{dp}{dx}$$

and

$$J_n = q n \mu_n E + q D_n \frac{dn}{dx}$$

are the hole and electron current densities represented by the usual drift and diffusion components in both the oxide and the semiconductor. The values of mobility used in the oxide are 20 cm²/V s for electrons and 10⁻⁵ cm²/V s for holes.^{5,6} Both hole and electron traps are modeled as single-energy-level traps with trap densities N_{Tp} and N_{Tn} . The cross sections σ_n and σ_p are typically 10⁻¹⁵ and 10⁻¹⁸ cm².⁷ The value of hole cross sections here used are lower than the values reported in the literature.^{7,8} This is because we have used v_{th} (the thermal velocity) instead of v_d (the drift velocity) in the trap rate equation. This point is discussed in more detail in a later section. τ_p and τ_n are the detrapping time constants, taken to be a few thousand seconds. In addition, in the case of electrons, recombination with trapped holes is also considered. G_{ox} is the effective generation rate in the oxide after geminate recombination. Geminate recombination is taken into account using the curve of yield as a function of electrostatic field calculated by Ausman.⁹ The net generation rate is obtained at each point in the oxide after multiplying this yield by the generation rate obtained from the dose rate. For the semiconductor, the usual Shockley-Read-Hall model of recombination is used.

It was found that the solutions in the oxide were the same whether or not the continuity equations were solved

in the semiconductor. This is due to the large barrier which prevents injection of holes and electrons from silicon into the oxide. So most of the simulations were performed just solving the Poisson equation throughout the structure and all five equations in the oxide, i.e., the quasi-Fermi levels in the silicon were assumed to be the same as the equilibrium fermi level.

The boundary conditions used were the following. For the SiO₂-metal contact, two boundary conditions were tried out. The first was a Dirichlet condition, where an ohmic contact was assumed, i.e., $\psi = V_{\text{appl}}$ and n and p were maintained at their equilibrium values. Since the equilibrium values of carrier concentrations in the oxide are almost zero, errors in the values of the density of states in the oxide, which are not known exactly, are negligible. The second condition tried out was a Neumann condition with $J_n = qn\mu_n E$, $J_p = qp\mu_p E$, and $\psi = V_{\text{appl}}$. This is valid only under high-field conditions when the drift current dominates. The solutions obtained in the two cases differ only in the first 20–30 Å near the metal-SiO₂ contact. This makes sense as this process is really a bulk-limited rather than a contact-limited process.

At the Si-SiO₂ interface, Gauss' law was directly used instead of the Poisson equation. Also, the quasi-Fermi level was assumed to be continuous at the interface. For a structure in which the material properties vary gradually from one material to another, the interface is gradual and the quasi-Fermi level is continuous. Since the almost abrupt Si-SiO₂ interface is the limiting case of such a structure, the quasi-Fermi level is assumed to be continuous across the interface. This abrupt change in material properties at the interface leads to large quasi-electric fields, which bring the electron and hole concentration at the oxide end of the interface close to their equilibrium values. This has also been observed in the numerical simulations. The silicon-metal contact is assumed to be an ohmic contact.

Since the structure is modeled as a heterojunction, the vacuum level is used to represent the electrostatic potential, with the equilibrium Fermi level used as the reference. The finite difference method was used in order to discretize the equations, with the Scharfetter-Gummel discretization technique¹⁰ for the continuity equations. Both the backward Euler as well as the second-order Gear's method were tried out for the time discretization. Since radiation is usually incident for a few hours, the second-order Gear's method with nonuniform time steps¹¹ provided a significant improvement in simulation times. Typically, the time required for simulation was halved by the use of this method. The algorithm for time steps was based on the local truncation error, and is similar to the one used in Ref. 11.

III. RESULTS OF THE SIMULATION

For the simulation, we used a Gaussian distribution of traps with various centroids and standard deviations. First, simulations carried out without electron trapping are presented. Figure 1 shows some typical curves of flat-band voltage shifts (ΔV_{fb}) as a function of time, or equivalently, dose. These results were obtained for a dose rate of 100 rad

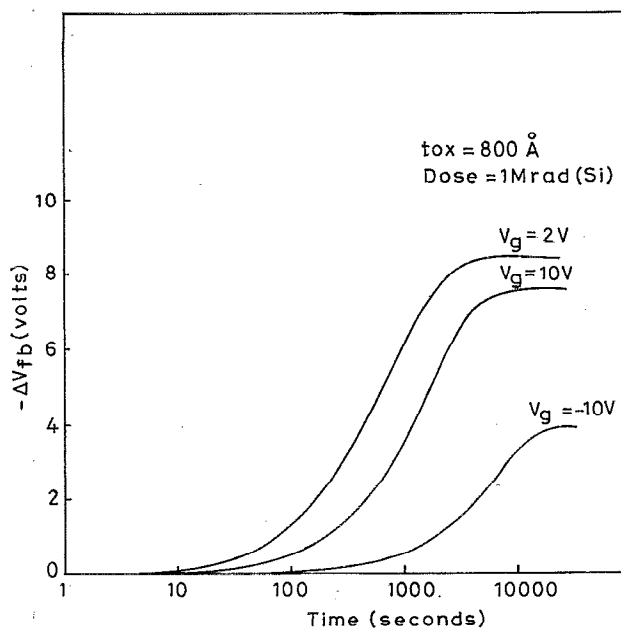


FIG. 1. Variation of flat-band shift ΔV_{fb} with time for $V_g = -10, 2,$ and 10 V.

(Si)/s, with a peak trap density of about $10^{18}/\text{cm}^3$. The oxide thickness was 800 Å and the centroid was at about 100 Å from the Si-SiO₂ interface. As expected, ΔV_{fb} initially increases with dose, and finally saturates when the trapping and detrapping rates become equal. In this case, the detrapping time constant used was 10 000 s, giving rise to low detrapping rates. The low detrapping rates result in a dynamic equilibrium being established when the trapping rates become small, i.e., when the traps are almost completely filled. The saturation level as well as the rate of buildup of charge depends on the gate voltage, as the free-hole concentration changes with the applied field.

Figure 2 shows a log-log plot of ΔV_{fb} versus the oxide thickness (t_{ox}) for a total dose of 1 Mrad (Si) for various gate voltages. It is seen that ΔV_{fb} shows a linear-to-cubic variation with oxide thickness. The linear variation occurs at larger thicknesses. This is because at larger thicknesses there is a large number of free holes in the oxide both due to lower fields for the same voltage and a larger total number of generated holes. This leads to higher trapping rates and the traps quickly get almost completely filled. Further increase in the oxide thickness makes no difference to the amount of trapped charge. Since most of the traps are concentrated near the interface, the capacitance of the trapped charge leads to a linear variation of ΔV_{fb} with t_{ox} . At medium thicknesses, the traps never get completely filled and trapping is limited by the total number of holes generated in the oxide. When the thickness increases, ΔV_{fb} increases not only due to the capacitance of the trapped charge, but also because the total number of holes increases with thickness, giving a t_{ox}^2 dependence. At still lower thicknesses, the field in the oxide is very large for the same applied voltage. Now the drift velocity of holes is fairly large and a greater number of them tend to get swept

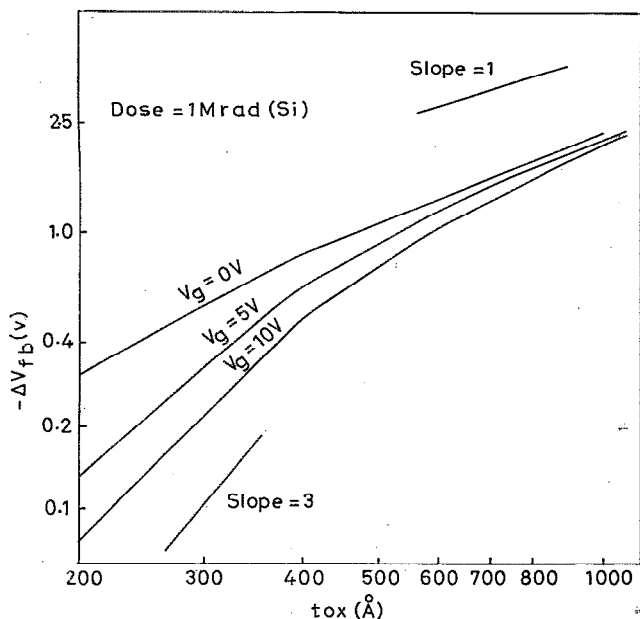


FIG. 2. Dependence of ΔV_{fb} on the oxide thickness t_{ox} for $V_g = 0, 5,$ and 10 V.

out of the oxide before getting trapped. So for these thicknesses, there is yet another t_{ox} dependence due to the fact that for larger thicknesses, the total number of holes increases due to lowered fields besides the increase due to a larger number of generated holes. These results are in general agreement with the analytical results of Viswanathan and Maserjian,¹ who have predicted a t_{ox}^2 -to- t_{ox}^3 dependence of ΔV_{fb} on oxide thickness. However, it should be noted that they have used a uniform trap density in the oxide and the drift velocity of holes instead of the thermal velocity in the trap rate equation. The use of v_d in the trap rate equation reduces the field dependence of the trapping rate and hence decreases the thickness dependence. If v_{th} is used by us along with a uniform trap density, a t_{ox}^2 -to- t_{ox}^4 dependence will be obtained.

Figure 3 shows the variation of ΔV_{fb} with gate voltage (V_g) for two thicknesses for a total dose of 1 Mrad (Si). For positive gate voltages, ΔV_{fb} rises sharply, goes through a maximum, and then begins to fall. This is because when the gate voltage increases beyond the oxide flat-band condition, more and more holes are driven to the interface, leading to a rise in the flat-band voltage shift. ΔV_{fb} continues to rise until it reaches a point when the increase in the hole concentration at the interface due to a positive gate voltage is offset by a decrease in the hole concentration due to high electric fields. Since the electric fields are lower for larger thicknesses at the same gate voltage, this maximum occurs at larger voltages for higher oxide thicknesses. This decrease of ΔV_{fb} is commonly observed in experiment and it has been previously attributed to a reduction in capture cross section with the electric field. However, our simulation shows that lower cross sections are not the sole reason for a decreasing ΔV_{fb} at higher fields. The decrease could be simply due to the fact that holes are swept out of

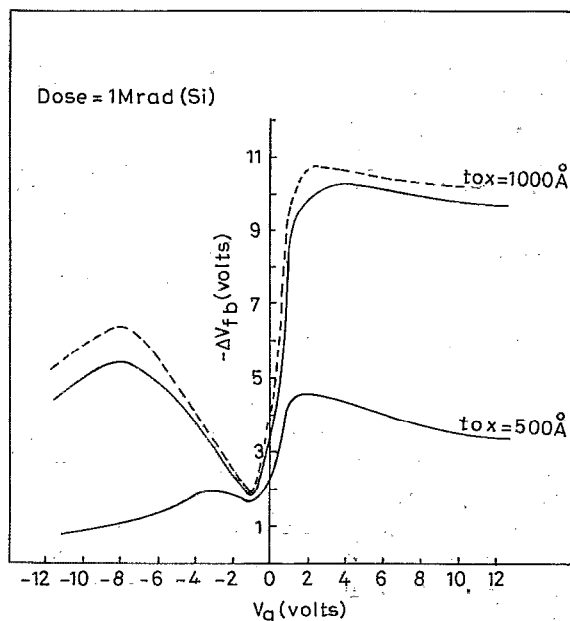


FIG. 3. ΔV_{fb} vs gate voltage V_g for $t_{ox} = 500$ and 1000 Å. The dashed line shows ΔV_{fb} obtained without geminate recombination.

the oxide faster at higher fields. This decrease will continue up to fairly large fields, as the mobility measurements of holes show almost a constant mobility up to 5.5 MV/cm,⁶ with no signs of velocity saturation.

With negative voltages, ΔV_{fb} shows a similar decrease at large negative voltages. In addition, beyond a certain amount of trapped charge, the flat-band voltage shift goes through a minimum near the oxide flat-band voltage. This is because when the trapped charge exceeds a certain value, the oxide bands become concave upwards as indicated in Fig. 4, which shows the potential profile across the oxide.

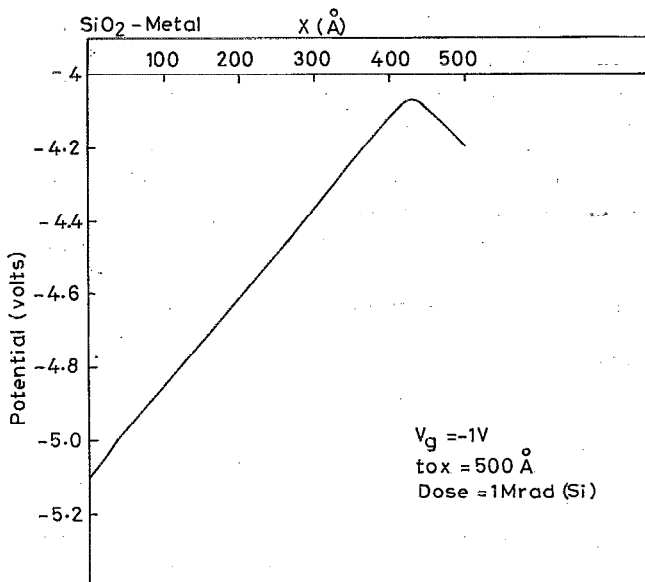


FIG. 4. Electrostatic potential as a function of position in the oxide for $V_g = -1$ V and a total dose of 1 Mrad(Si).

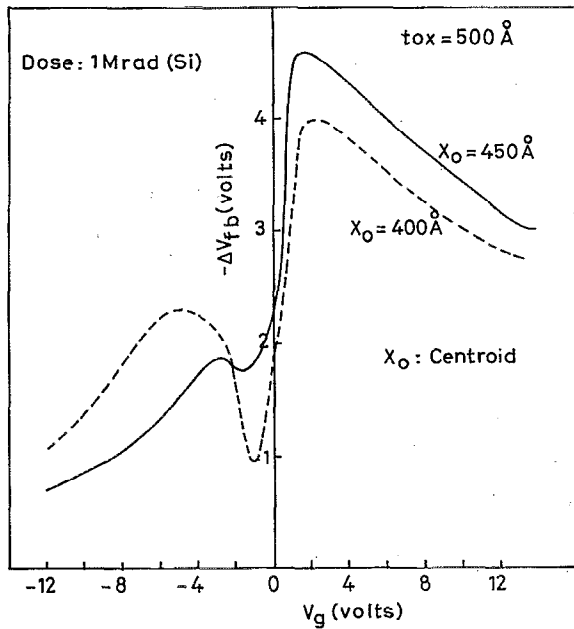


FIG. 5. ΔV_{fb} vs V_g for $t_{ox} = 500 \text{ \AA}$. The solid line is obtained with the centroid of the trap distribution at 50 \AA and the dashed line is obtained with the centroid at 100 \AA from the Si-SiO₂ interface.

The peak of the trap density is located approximately at the point where the potential is a maximum. So the holes generated in the oxide tend to move away from the traps leading to low values of ΔV_{fb} .

Figure 3 also shows a curve (dashed line) without geminate recombination which also goes through this minimum near-zero oxide fields. This suggests that it is the change in the band structure caused by the trapped charge that causes this minimum and not geminate recombination as previously assumed. It is to be noted that although the yield is very low at low fields, zero field is almost never obtained throughout the oxide due to the large fields created by the trapped charge itself. However, at these low fields the initial trapping rate is very low and it takes a long time for the trapped charge to build up. Figure 5 shows the effect of shifting the centroid away from the Si-SiO₂ interface. It is seen that the ratio of the average ΔV_{fb} at positive voltages to the average ΔV_{fb} at negative voltages decreases. This is expected because for a positive voltage, the hole concentration increases towards the interface leading to larger trapping rates when the centroid is shifted towards the interface. But for negative voltages, the hole concentration reduces towards the interface, reducing the amount of trapped charge as the centroid is shifted towards the interface.

Figure 6 shows a simulation in which electron traps have been included. The simulation was done using an oxide thickness of 400 \AA , with the centroid of the hole trap distribution at 80 \AA and the centroid of the electron trap distribution at 120 \AA from the Si-SiO₂ interface. Curve (a) was obtained without electron traps and curve (b) was obtained for the same conditions with nearly equal electron and hole trap densities. It is seen that the addition of elec-

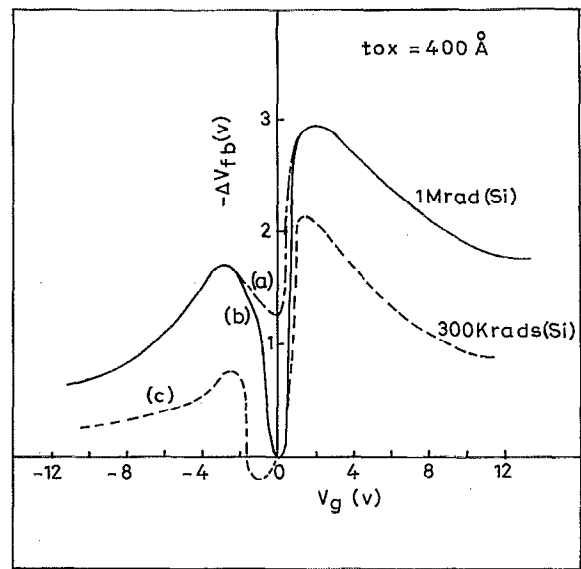


FIG. 6. Dependence of ΔV_{fb} on V_g for $t_{ox} = 400 \text{ \AA}$ when electron traps are included. Curve (a) is obtained without electron traps for a total dose of 1 Mrad(Si) , (b) is obtained with nearly equal electron and hole trap density using the same conditions as for (a), and (c) is obtained with an electron trap density an order of magnitude higher than the hole trap density for 300 krad(Si) .

tron traps significantly alters ΔV_{fb} at near-zero fields in the oxide. Elsewhere the electron traps have no effect on ΔV_{fb} . This is due to the relatively large mobility of electrons ($20 \text{ cm}^2/\text{V s}$ as compared to $10^{-5} \text{ cm}^2/\text{V s}$ for holes) which leads to low electron concentrations in the oxide except when the field is low. At $V_g = 0 \text{ V}$, ΔV_{fb} is positive indicating a greater shift due to electrons. Figure 7 shows the buildup of charge in the oxide with time for this case. It is seen that after increasing for a considerable

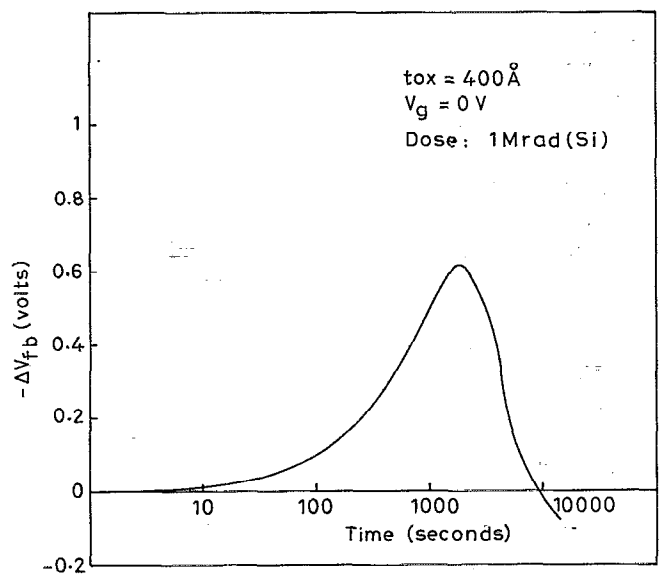


FIG. 7. ΔV_{fb} as a function of time for $t_{ox} = 400 \text{ \AA}$, total dose = 1 Mrad(Si) , and $V_g = 0 \text{ V}$. This curve is obtained using almost equal electron and hole trap densities.

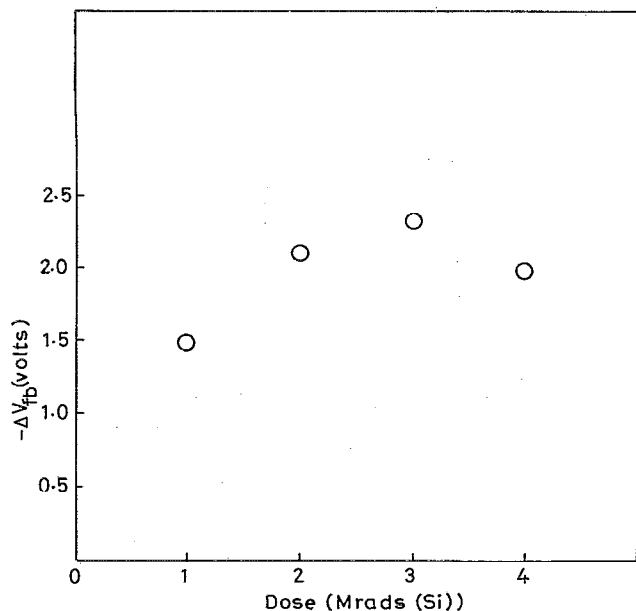


FIG. 8. ΔV_{fb} vs time obtained experimentally for nitrated oxides with 30-min nitridation in 25% NH_3 at 1000°C (see Ref. 13).

amount of time, ΔV_{fb} begins to fall and eventually becomes positive. This decrease begins to occur when the field due to the trapped charge compensates for the applied and built in oxide field. If the positive charge builds up further, the oxide bands become concave with the potential minimum for electrons located near the centroid of the hole traps which is near the centroid of the electron traps. Beyond this dose, electrons generated throughout the oxide move towards the minimum energy point of the conduction band and get trapped, thus compensating for the positive charge. Curve (c) in Fig. 6 shows ΔV_{fb} vs V_g when the electron trap density is an order of magnitude larger than the hole trap density for a total dose of 300 krad (Si). Here it is seen that ΔV_{fb} is positive around $V_g = -1$ V, which is around the flat-band condition for the oxide. Due to large electron trap densities ($10^{20}/\text{cm}^3$) and capture cross sections, the electrons, which have near-zero drift velocities at this voltage, tend to get trapped easily leading to a positive ΔV_{fb} .

The reduction of ΔV_{fb} beyond a certain dose has been observed in our laboratory for nitrated oxides.^{12,13} A typical variation of ΔV_{fb} with dose for nitrated oxides¹³ is shown in Fig. 8. So, contrary to conclusions drawn by Dunn,¹⁴ we believe that electron traps can compensate for the flat-band voltage shifts produced by holes if the applied field is low or the band structure is dictated by the trapped holes and the centroid of the electron traps is near that of the hole traps.

IV. COMPARISON WITH EXPERIMENT

Figures 9 and 10 show a comparison of our simulation results with experiments performed in our laboratory for pyrogenic oxides,¹⁵ and it is seen that a fairly good fit is obtained. Figure 11 shows the comparison of simulation

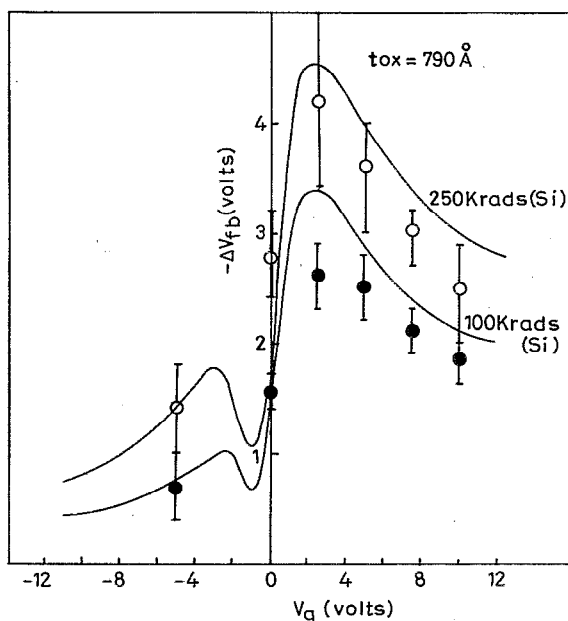


FIG. 9. Comparison of simulated curve with experimental data for a 790-Å pyrogenic oxide. (●) is the data for 100 krad(Si) and (○) is the data for 250 krad(Si). Data from Ref. 15.

results with data reported by Fleetwood *et al.*¹⁶ In this case the values of trap density needed to fit data at higher doses were higher, being $10^{18}/\text{cm}^3$ at 55 krad and $5 \times 10^{18}/\text{cm}^3$ at 925 krad. This seems to indicate that there is some amount of trap generation taking place. This is quite probable since the dose rates used by them are quite large (1 Mrad/h).

It is seen that the results of the simulation compare fairly well with experimental data, although the model itself has some limitations. We have assumed a simple drift-

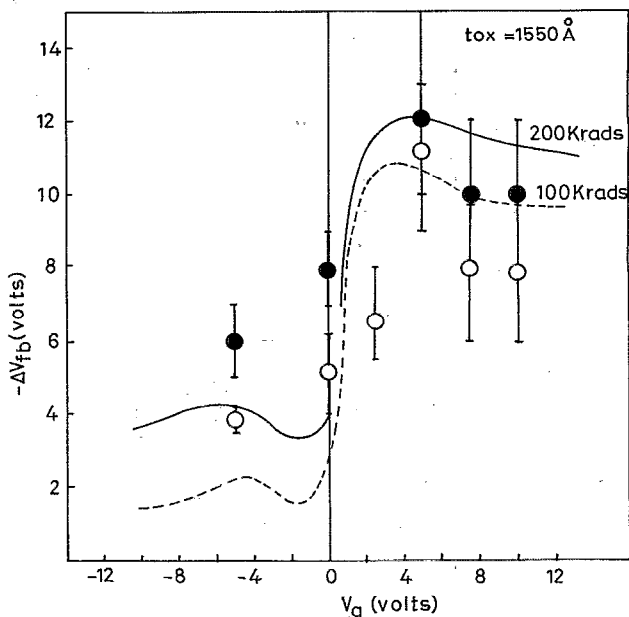


FIG. 10. Comparison of simulated curve with experimental data for a 1550-Å pyrogenic oxide. Data from Ref. 15.

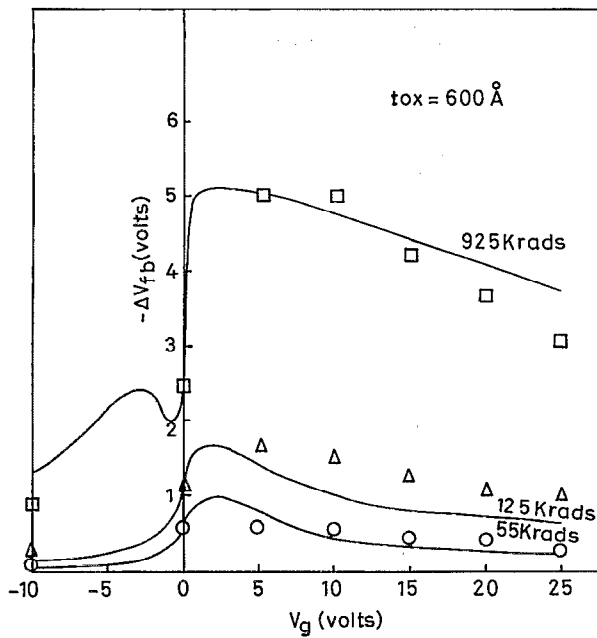


FIG. 11. Comparison of simulated results with data obtained by Fleetwood *et al.* (see Ref. 16).

diffusion model for hole transport in the oxide, whereas the actual transport mechanism is believed to be more nearly described by the CTRW model. Also, velocity saturation of electrons has not been taken into account. However, as seen from Fig. 6, this will not alter the results significantly as electron traps play a significant role only when the field in the oxide is nearly zero, much below the fields required to produce velocity saturation.

Typical values of data used to fit the experimental data are $N_T = (1-6) \times 10^{18}/\text{cm}^3$, $\sigma_p = 10^{-18} \text{ cm}^2$, $\sigma_n = 10^{-15} \text{ cm}^2$, and $\tau_{p,n} = 10\ 000 \text{ s}$. These are typically the values reported in the literature.^{7,8} In the case of hole capture cross section the value reported in the literature is scaled by a factor of v_d/v_{th} as those values were obtained assuming $v_d = v_{th}$. In our opinion, the use of drift velocity in the trap rate equation for holes is not justified. It is probably valid for electrons, which due to their relatively large mobility attain a saturation drift velocity, which is numerically equal to the thermal velocity. This is not true for holes which have a very low almost constant mobility up to 5.5 MV/cm.⁶ The use of a "thermal velocity" is also supported by the fact that our simulations compare well with experiment. Some of the results like the cubic variation of ΔV_{fb} with oxide thickness will not be obtained if the drift

velocity is used instead of the thermal velocity and all the traps are concentrated near the interface. This is simply seen by noting that when the field increases, the concentration of holes reduces, reducing the trapping rate, but the drift velocity increases increasing the trapping rate. The observed field dependence of σ_p , which is measured using $v_d = v_{th}$,^{7,8} may occur partly because the drift velocity itself changes with the field. However, the use of thermal velocity may not be correct as the holes in SiO₂ are believed to exist not as free particles, but as trapped charge in shallow traps above the valence band. In order to avoid this uncertainty, we have kept the capture probability ($= \sigma_p v_{th}$) constant and equal to the measured capture probability at a particular field.

V. CONCLUSIONS

In this paper we have presented a numerical model for positive-charge buildup in MOS structures under irradiation. The results of the simulation agree reasonably well with experiment. The model also provides a lot of physical insight into the nature of charge buildup in the oxide under irradiation.

ACKNOWLEDGMENT

This work was partially funded by the Department of Electronics, Government of India.

- ¹ C. R. Viswanathan, and J. Maserjian, *IEEE Trans. Nucl. Sci.* **NS-23**, 1540 (1976).
- ² J. N. Churchill, T. W. Collins, and F. E. Holmstrom, *IEEE Trans. Electron Devices* **ED-21**, 768 (1974).
- ³ J. N. Churchill, F. E. Holmstrom, and T. W. Collins, *J. Appl. Phys.* **50**, 3994 (1979).
- ⁴ J. N. Churchill, F. E. Holmstrom, and T. W. Collins, in *Advances in Electronics and Electron Physics* (Academic, New York, 1982), Vol. 58, p. 1.
- ⁵ N. F. Mott, *Adv. Phys.* **26**, 363 (1977).
- ⁶ R. C. Hughes, *Phys. Rev. B* **15**, 2012 (1975).
- ⁷ F. B. Mclean, H. E. Boesch, Jr., and T. R. Oldham, in *Ionizing Radiation Effects in MOS Devices and Circuits*, edited by T. P. Ma and P. V. Dressendorfer (Wiley-Interscience, New York, 1989), p. 87.
- ⁸ M. Aitken and D. R. Young, *IEEE Trans. Nucl. Sci.* **NS-24**, 2128 (1977).
- ⁹ G. A. Ausman, Jr., Report HDL-TR-2097, Harry Diamond Laboratories, 1987.
- ¹⁰ D. L. Scharfetter and H. K. Gummel, *IEEE Trans. Electron Devices* **ED-16**, 64 (1969).
- ¹¹ H. Shichman, *IEEE Trans. Circuit Theory*, **CT-17**, 378 (1970).
- ¹² V. S. Kumar, M. Tech thesis, IIT, Bombay, 1990.
- ¹³ V. Ramgopal, M. Tech thesis, IIT, Bombay, 1991.
- ¹⁴ G. J. Dunn, *J. Appl. Phys.* **65**, 4879 (1989).
- ¹⁵ S. A. Rajababu, M. Tech thesis, IIT, Bombay, 1990.
- ¹⁶ D. M. Fleetwood, P. V. Dressendorfer, and D. C. Turpin, *IEEE Trans. Nucl. Sci.* **NS-34**, 1178 (1987).